

# Investigation of Taper Profile in Development of Compact Tapered Slot Microstrip Antennas for X-Band SATCOM Applications

Emrah Uğurlu<sup>1, \*</sup> and S. Sinan Gültekin<sup>2</sup>

**Abstract**—In this paper, four novel wide-band dual tapered slot (DTS) microstrip antennas (MSAs) are proposed for X-Band Satellite Communications (SATCOM) applications. Three of them have stripline feed insertion between SMA connector and tapering profile, whereas the fourth one omits the stripline feed insertion. Each antenna is fed with a coaxial connector from one face and consists of conductors on each side of an FR-4 substrate, which increase gradually towards the edges. The aim is to design receiver antennas capable of operating in X-Band Satellite Communications (7250–7750 MHz) range and investigate the effects of tapering profiles on the performance. For this purpose, each antenna is defined in terms of parameters, and the optimum values for all parameters are calculated using High Frequency Structure Simulator (HFSS) software. The antennas are simulated and practically fabricated. Results show agreement between simulations and measurements. The antennas have impedance bandwidth of 380 MHz centered at 7448 MHz for dual linearly tapering, 540 MHz centered at 7434 MHz for dual circularly tapering, 900 MHz centered at 7555 MHz for dual exponentially tapering, within the aimed Super High Frequency (SHF) range. Also, the designed fourth antenna having dual circularly tapering without the stripline feed insertion has a bandwidth of 1150 MHz centered at 7676 MHz. It is proposed that taper profile affects bandwidth, gain, radiation efficiency, radiation pattern and antenna dimensions.

## 1. INTRODUCTION

Large bandwidth requirements brought up by the recent advances in satellite and wireless communications increase the popularity of designing antennas capable of operating with large bandwidths. Just as bandwidth, antenna weight is another major factor for airborne or space platforms, where size, weight and balance are crucial. The ease of fabrication can be counted as a third factor to be considered in antenna design. MSAs are very popular in many airborne and space research activities with their features as low weight and low fabrication costs. Initially, the early MSA designs had narrow bandwidths, but today MSAs have large bandwidths by utilizing various approaches, such as using tapered slot designs or improving the impedance matching at feed line by various transition forms [1–12].

One of the above mentioned designs is called Tapered Slot Antennas (TSAs), which have wide bandwidths and light weight, making them good candidates for airborne and space applications. Besides, manufacturing process for TSA is practical and cheap.

Currently, there is a growing demand in obtaining wideband high data rate for beyond-line-of-sight (BLOS) communications on mobile platforms, especially for military applications. However, there are a few concerns to be addressed on mobile platforms. The first concern is the mobility of the platform. If reception of the signals from a wide variety of directions is required on a platform as an aircraft, then either the main beam should be adjustable or lower directivity antennas should be used. Because during the maneuvers, the antenna on the mobile platform can be in many orientations relative to the

---

*Received 2 July 2016, Accepted 11 October 2016, Scheduled 30 October 2016*

\* Corresponding author: Emrah Ugurlu (eugurlu@rocketmail.com).

<sup>1</sup> 131st AEW&C Group Command, Turkish Air Force, Konya, Turkey. <sup>2</sup> Department of Electrical & Electronics Engineering, Faculty of Engineering, Selçuk University, Konya, Turkey.

satellite (although reception is mostly from top direction), and the signal is expected to be received from a wide angular volume.

Another concern is the movement of the satellites. Even the geostationary orbit satellites do not remain exactly stationary in their orbits; rather they vary inside a small box, called stationkeeping box  $\pm 0.1^\circ$  along *N-S* and *E-W* directions. The main beams of large antennas are smaller than the stationkeeping box. Therefore, to maintain line-of-sight, a steering and tracking system is required. On the other hand, small antennas have larger main beams, so it is easier for them to point at a satellite continuously. So, practical limits on the gain or directivity of antennas are dominated by the requirement to maintain the beamwidth large enough to cover the desired angular volume.

To satisfy broadband communication needs on mobile environments, there are mainly two approaches. The first one uses high gain scanning antennas such as electronically scanned phased arrays. These systems have high directivity and to keep pointing towards a specific satellite. Their beamshape is adjusted electronically, rather than mechanically. However, these scanning antennas are hardly cost-effective, because of either weight or aerodynamic considerations on air platforms. TSAs can be used to implement electronically scanned phased arrays, with their low profiles and lightweight properties. The second approach, is using low directivity antennas. Their radiation patterns may not be ideally omnidirectional but should be wide enough to maintain continuous satellite coverage.

For space platforms, additional issues have to be addressed. For example, satellites on lower earth orbits have specific elevation requirements, which may be critical for designs. In NASA's Space Technology 5 (ST5) mission [13], the gain pattern required is greater than or equal to  $-5$  dBi at elevations of interest, which are between  $0^\circ$  and  $40^\circ$ . The satellite has highly elliptical low earth orbit and elevation angle relative to the ground changes. There is a relationship between maximal elevation and communication duration. Higher maximal elevation means longer communication between satellite and ground terminals, as shown in Figure 1. In this case, wider elevation range is desirable.

The implementation of MSAs in airborne platforms dates back to 1973 when Weinschel designed MSAs that can be used in S-band communication on rockets [16]. Later, the potential usages of MSAs in space applications were discovered, and conformal antenna arrays for L-band communication between KC-135 tanker aircrafts and ATS-6 satellite were presented [17]. The next application of TSAs on satellite communications was performed by Simons et al. with a linearly tapered slot antenna that can operate in 8–32 GHz frequency band [18]. They investigated return losses and radiation patterns of their designs in X/Ka-Bands and managed to achieve one of the largest bandwidths with their work. A relatively recent research on X-band communications was carried out by Lekshmi and Raglend [19]. They examined the taper profile parameters of a linearly tapered slot antenna which was aimed to operate in 11–14 GHz frequency band. They claimed that increasing the slot width decreased the return loss and side lobes while increasing the gain and main lobe in the radiation pattern. Today, the effects of taper profile on antenna performance is still an important topic under investigation.

In TSAs, the style of the gradual increase between conductors is called tapering profile. After the first TSA was introduced by [1], various tapering profiles were studied. Exponential tapering profile was proposed by [2], which is also known as Vivaldi. Linear taper profile was proposed by [3]. Both

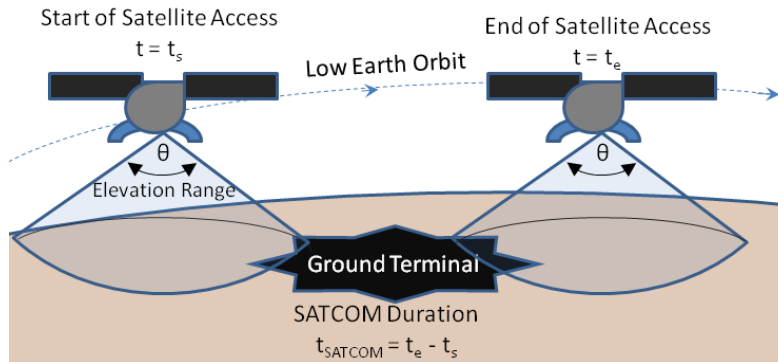


**Figure 1.** Maximal elevation and communication duration relationship.

studies obtained wide bandwidths. Vivaldi type was followed by antipodal [4] and balanced antipodal [5] Vivaldi versions. By introducing balanced antipodal version of Vivaldi, it was shown that conductors on both sides of the tapered slots could function as ground. Later, researchers examined the effect of taper profile on antenna performance. In [6], a correlation between radiation beam width and taper profile was presented. It was followed by the introduction of dual exponential tapering profile by Lee and Livingston [15]. The conductors on both faces were resembling curved microstrip lines, in which one of them functioned as ground. Another study regarding taper profile was a composite tapering profile, which was proposed in [7]. By combining high tapering and low tapering profiles into a single curve, gain performance was improved in comparison to a classical Vivaldi type antenna. Since the early designs of TSAs, the importance of bandwidth on the transition from microstrip to slotline has been known. To improve the bandwidth of these kinds of transitions, various techniques, such as using balun transitions [8], circular stubs [9] and radial [10] stubs, were applied. Even today, transition from microstrip to slotline is important and should be taken into account in TSA designs. The above studies laid out the fundamentals of TSAs. Later, the researchers worked on optimizing TSAs. For example, in [11] parametric analysis and design of Vivaldi antenna arrays was presented. In order to do this, first, the antenna is defined in terms of parameters; then the effects of these parameters on the design are examined.

As the computational power of computers are increased, and electromagnetic simulators are improved, evolutionary antenna design and optimization field has gained much popularity, and many antenna types are investigated. In 2006, NASA's ST5 mission was launched into space using an unusual shaped X-band antenna, which was optimized by Genetic Algorithm, as one of its antennas. This evolved antenna was the first computer-evolved antenna deployed in space [13, 14]. Similar approaches were followed in evolutionary TSA designs. Optimization of TSAs was accomplished by [12], in order to manufacture a balanced antipodal Vivaldi antenna for ultra wideband applications using FR4 material.

In this study, four novel wide-band tapered slot antennas are proposed for X-Band Satellite Communications applications. All of the antenna structures consist of two microstrip lines on each side of an FR-4 substrate, resembling antipodal versions of Vivaldi. But taper profile is dual linear, dual circular and dual exponential where the radiating elements are curved microstrip lines with no conductors other than the tapering regions. Also, with the symmetric nature and dual taper profile of the designed antennas, two different levels of tapering are achieved for a single antenna. Each antenna is fed with coaxial connector from one face. The symmetry of the antennas and newly introduced semi-annular stubs on both sides of SMA connectors made the transition from microstrip to slotline easier. By finding the optimum values for each parameter, matching is obtained for  $50\ \Omega$  coaxial feed in 7270–7652 MHz range for linearly tapered, 7100–7620 MHz range for circularly tapered and 6830–7780 MHz range for exponentially tapered profiles. Also, a fourth circularly tapered antenna, which has wider beamwidth and reduced dimensions, is designed in 7280–8430 MHz range. The parameters of the antennas and optimization process are explained in the following section.

## 2. MATERIALS AND METHODS

The geometries of the designed dual linearly, dual circularly and dual exponentially tapered antennas are given in Figure 2(a), Figure 2(b) and Figure 2(c), respectively. Each antenna consists of two conductors on both faces of an FR-4 dielectric substrate. The figures show both of the conductors seen from one side, as if the substrates are transparent. The orange color shows top conductors, and the yellowish color shows bottom conductors. On the sides of the substrate, the conductors are separated from each other, resembling a Y shape.

The taper profile of each conductor is determined by two parameters,  $a$  and  $b$ .  $a$  is the distance of the conductor in horizontal direction, from the starting point of taper to the edge.  $b$  is the vertical distance of conductor, from the bottom edge of the feed to the closer edge of the conductor. To reduce the fringe effect on the tips of the conductors, the tips are rounded by adding a semi-circular part, whose diameter is the same as the width of the conductor ( $w$ ) for linear and circular tapering. However, for the exponential case, it is omitted, because it would be difficult to add the semi-circular part smoothly, without creating any discontinuity.

The substrate dimensions are determined with respect to the conductor dimensions (as great as

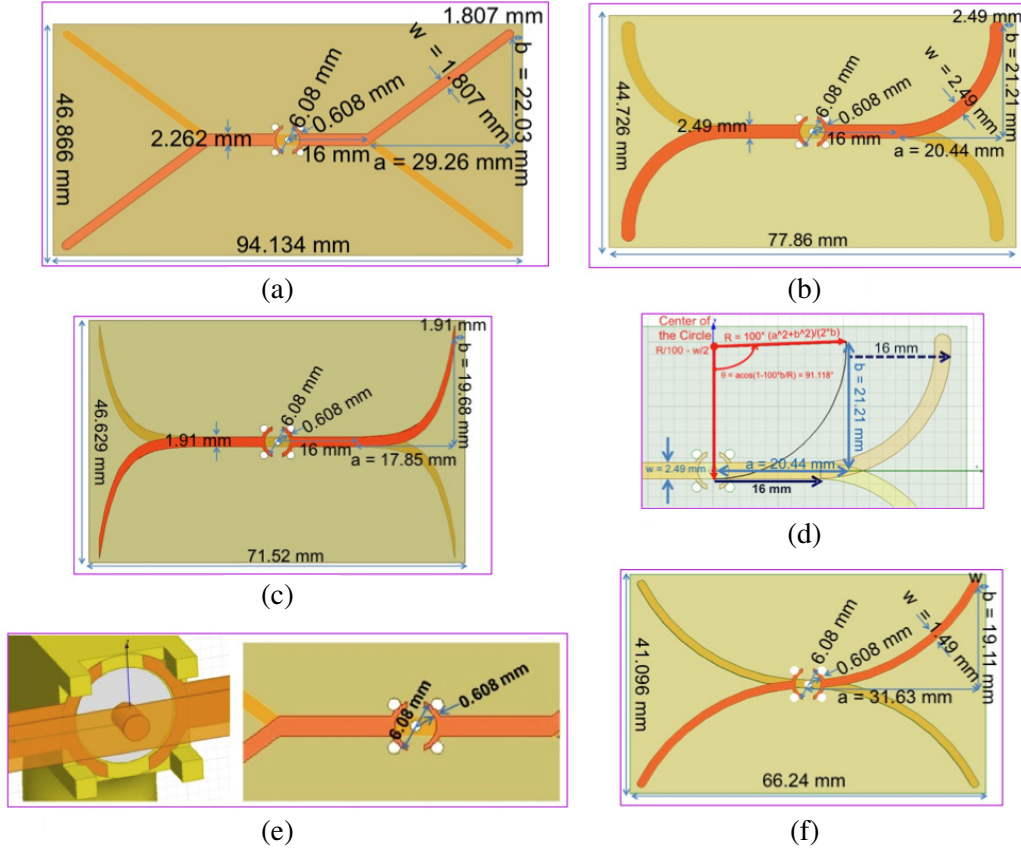


**Figure 2.** Geometry of DTSAAs. (a) DLTSA, (b) DCTSA, (c) DETSA, (d) DCTSA taper parameters, (e) SMA connection to semi-annular stubs, (f) DCTSA without 16 mm feed.

**Table 1.** Exponential taper rate parameters.

Parameter	Evaluated Value
$X(-t)$	$-t$
$Y(-t)$	$-w/2 + (b + w/2 * (1 - 100 * b/R)) * (\exp(300 * -t) - 1)/(\exp(300 * a) - 1)$
Start $-t$	0
End $-t$	$a$

one conductor width on both sides). As a result, all the designed antennas can be defined using three parameters:  $a$ ,  $b$  and  $w$ . For the circular and exponential tapering, the tapering rate is also determined by  $a$  and  $b$ . For the dual circularly TSA (DCTSA) tapering rate parameters are given in Figure 2(d). For dual exponentially TSA (DETSAs) tapering rate parameters are given in Table 1.

Each antenna is fed using an SMA connector. SMA connectors have five pins, one in the middle and four at the outer corners. The outer pins of SMA connector are soldered to the stubs. The inner pin of SMA is soldered to the bottom conductor. To improve the matching of the transition from SMA to antenna, semi-annular stubs on two sides of the SMA are used on one face. The connection of SMA to the semi-annular stubs and the details are shown in Figure 2(e). The diameter of the stubs measured from the outer edges is 6.08 mm. The widths of the stubs are 0.608 mm.

Since the linear taper profile cannot start immediately from the centre (otherwise the outer pins of SMA and bottom conductor touches), a microstrip feed inserted before tapering begins, for all of the antennas. This microstrip feed insertion has a fixed length of 16 mm. However, the width of the feed is determined according to tapering conductors' width and profile, which are calculated by optimization

algorithm. Substrate height is 1.57 mm.

To optimize the parameters, first, the antennas have to be created as 3D objects in HFSS. Some of the antenna dimensions (circular stub diameter, circular stub width, microstrip feed length) have already been determined; however, the rest of the dimensions are defined in terms of the three parameters ( $a$ ,  $b$  and  $w$ ), which are to be optimized by built-in HFSS optimetrics tool. Genetic Algorithm (GA) is chosen as the optimization algorithm. The condition for cost calculation is chosen as “ $S_{11}$  value to be less than  $-10$  dB for  $7.5$  GHz”, which is the center of the  $7250$ – $7750$  range. Actually, there are other optimization targets for peak gain, Voltage Standing Wave Ratio (VSWR) and radiation efficiency. But during initial optimization trials, it is observed that  $S_{11}$  is the dominant parameter. Therefore, only  $S_{11}$  is used in the cost calculations. But at the end of the optimization, the designed antenna is verified to have a peak gain at least  $4$  dB, radiation efficiency at least  $60\%$  and VSWR less than  $2$  as design criteria.

First, DL TSA is optimized. Immediately after the first generation,  $S_{11}$  becomes less than  $-10$  dB. However, when  $S_{11}$  values versus frequency are plotted, it is seen that the centre of the pattern is located around  $7.6$  GHz and that the operational frequency range starts around  $7.48$  GHz, which means a shift in the pattern. At that point,  $-10$  dB criterion is changed to some deeper value, such as  $-40$  dB, for the rest of the optimization process to force the centre of the pattern to be at  $7.5$  GHz. The variations in  $S_{11}$  value at  $7.5$  GHz and plots in the whole range for some of the selected iterations are shown in Figure 3. Two of the iterations satisfy  $S_{11}$  value less than  $-40$  dB. One of them is obtained at the end of the GA optimization. The other one is obtained after the manual modification of the previous one, by manually truncating the decimal values of the parameters to be three decimal points at most (for example,  $w$  value is truncated from  $1.807452017$  to  $1.807$ ). This is required for the ease of fabrication and to make sure that the truncated values are still good, because even the small variations in parameters’ values change the results. The minimum-maximum range for each parameter, which is tried during optimization, is ( $0.635$  mm– $2.2$  mm) for  $w$ ; ( $15$  mm– $40$  mm) for  $a$ ; ( $15$  mm– $20$  mm) for  $b$ .

Secondly, optimization of DCTSA is done. The minimum-maximum range for each parameter, which is tried during optimization is ( $1.1$  mm– $2.5$  mm) for  $w$ ; ( $15$  mm– $40$  mm) for  $a$ ; ( $15$  mm– $25$  mm) for  $b$ . Thirdly, optimization of DETSA is done. The minimum-maximum range for each parameter, which is tried during optimization, is ( $0.635$  mm– $1.905$  mm) for  $w$ ; ( $15$  mm– $40$  mm) for  $a$ ; ( $15$  mm– $23$  mm) for  $b$ . The minimum-maximum ranges are determined by trial and error, because the iterations halt when the conductors touch a boundary, such as SMA legs or any part of the surrounding boundary condition on airbox. In addition to the antenna parameters, GA also has some parameters which affect the optimization. The parameters for the GA are given in Table 2. The number of individuals is chosen as  $5$ . This is mainly because of the computation time of a single iteration. The time to process cost calculation is very short for GA. However, to calculate  $S_{11}$  value and use it in cost calculation, first, an electromagnetic problem needs to be solved by HFSS. This increases the computation time for a

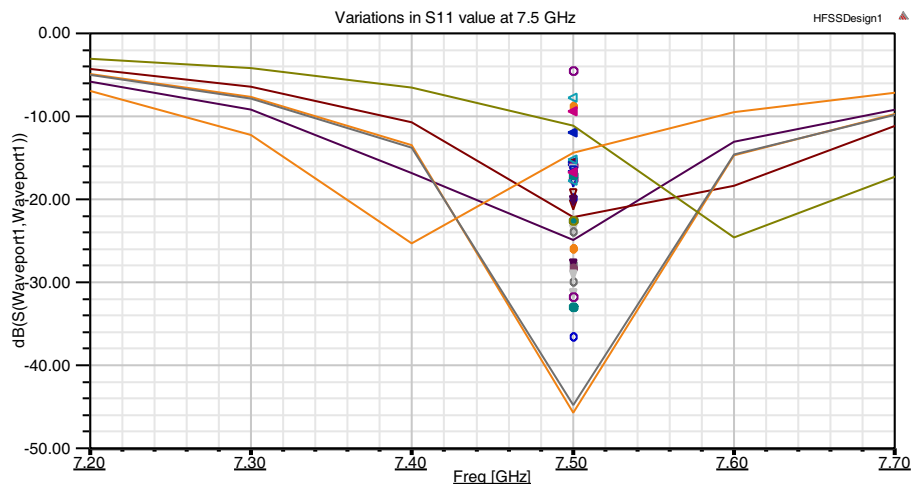


Figure 3.  $S_{11}$  variations in DL TSA simulations.

**Table 2.** GA parameters and their values.

Description	Option	Value
Parents	Number of individuals in Parents	5
	Roulette Selection Pressure in Parents	3
	Number of individuals in Mating Pool	5
Mating Pool	Crossover Type	Simulated binary crossover
	Individual Crossover Probability	1
	Variable Exchange Probability	0
	Variable crossover probability	1
	Mu	1
	Mutation Type	Polynomial Mutation
	Variable Mutation Probability	1
Children	Individual Mutation Probability	1
	Standard Deviation	0.05
	Number of Survivors in Children	3
Pareto Front	Number of Survivors in Parents	2
Next Generation	Number of individuals in Next Generation	5
	Roulette Selection Pressure	3

single iteration. For the linearly tapered antenna, to obtain the results of the optimization after nine generations, two days are needed with a quad-core 1.6 GHz 64 Bit PC with 6 GB RAM.

### 3. RESULTS

After the optimization, the obtained values for  $a$ ,  $b$ ,  $w$  and the total dimensions of the antenna are given as Table 3. The dimensions are also written in Figures 2(a)–(c). The simulation results regarding the peak gain, radiation efficiency,  $S_{11}$ , VSWR, radiation pattern are given in Figures 4(a)–(c).

These three antennas have  $-3$  dB beamwidths varying between  $20^\circ$  and  $40^\circ$ , which can be considered as narrow, and the way that they can be used for SATCOM applications is in arrays. This is according to the approach of implementing electronically scanning arrays. If the second approach of using low directional antennas is going to be pursued, these antennas are not adequate. It is assumed that the stripline feed from semi-annular stubs to the starting point of taper affects the beamwidth negatively. As a result, a fourth antenna is proposed, in which the 16 mm stripline feed insertion for DCTSA is omitted, and the taper profile starts immediately from the semi-annular stubs. The geometry of the designed circularly tapered antenna without the stripline feed insertion is given in Figure 2(e). The simulation results regarding the peak gain, radiation efficiency,  $S_{11}$ , VSWR, radiation pattern are given in Figure 4(d).

**Table 3.** Antenna physical parameters.

Type	Feed Width (mm)	Antenna Dimensions					Surface Area (mm <sup>2</sup> )	Reduction with respect to DLTSA
		$a$ (mm)	$b$ (mm)	$w$ (mm)	Total Width (mm)	Total length (mm)		
DLTSA	2.262	29.26	22.03	1.807	48.866	94.134	4600	0%
DCTSA	2.49	20.44	21.21	2.49	44.726	77.86	3482	24.3%
DE TSA	1.91	17.85	19.68	1.91	46.628	71.52	3335	27.5%
DCTSA2	1.49	31.63	19.11	1.91	41.096	66.24	2722	40.8%

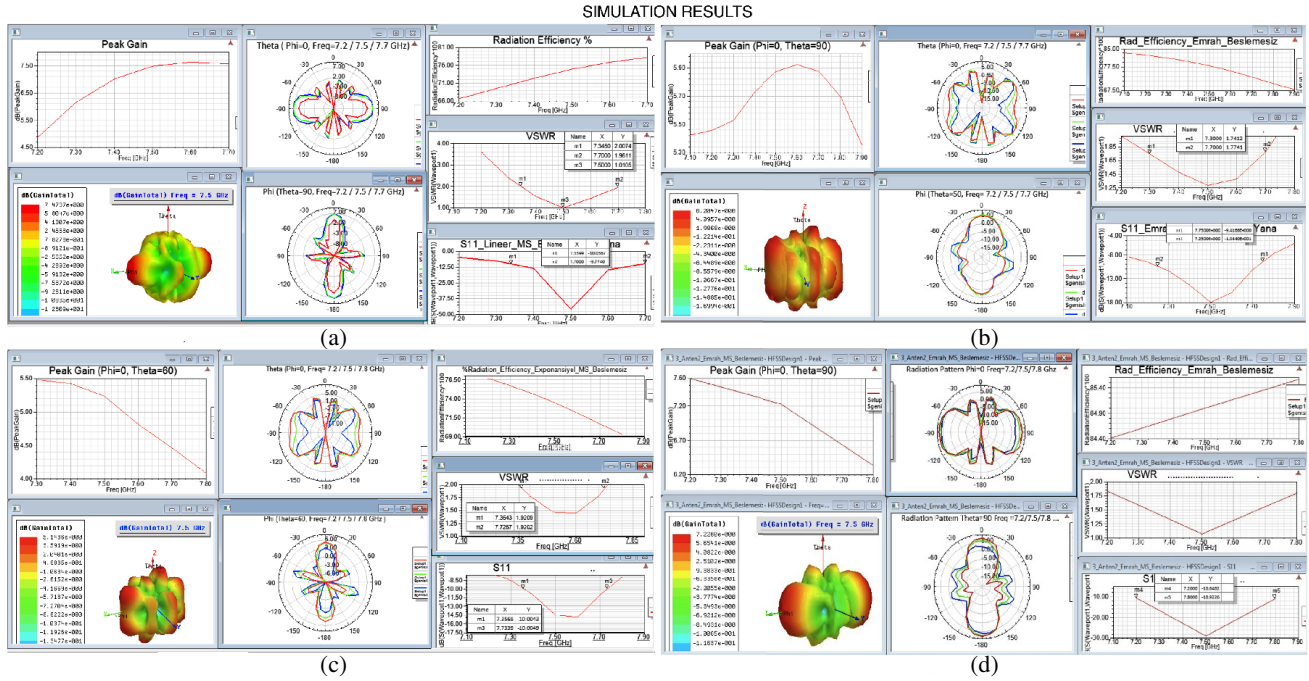


Figure 4. Simulation results obtained in HFSS after optimization. (a) DLTSA, (b) DCTSA, (c) DETSA, (d) DCTSA without 16 mm feed.

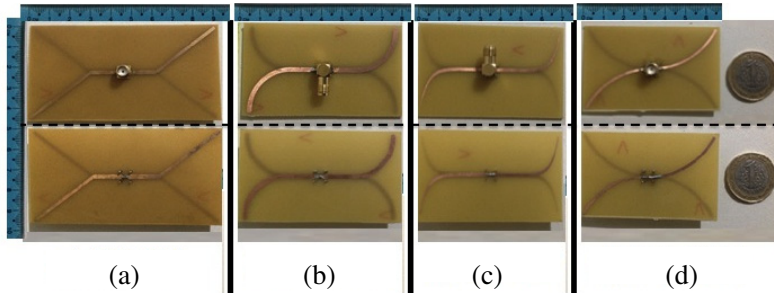


Figure 5. Manufactured TSAs (top and bottom views). (a) DLTSA, (b) DCTSA, (c) DETSA, (d) DCTSA2.

Table 4. Performance comparisons of the four antennas.

Type	Frequency Values (MHz)			Bandwidth (MHz)	$S_{11}$ (dB)	VSWR
	Lowest Frequency	Center Frequency	Highest Frequency			
DLTSA	7270	7448	7650	380	-30.05	1.065
DCTSA	7100	7434	7620	520	-30.75	1.059
DE TSA	6830	7555	7780	950	-32.85	1.047
DCTSA2	7280	7.676	8430	1150	-27.64	1.086

After obtaining satisfactory simulation results, fabrication is started. The manufactured antennas are shown in Figure 5.

As for the measurements, only  $S_{11}$  value and VSWR could be measured with the available equipment. The comparison of simulated and measured values for  $S_{11}$  and VSWR is given in Figure 6. Measured values for frequency range, bandwidth, centre frequency,  $S_{11}$  and VSWR are given in Table 4.

### 4. DISCUSSION

All the four antennas are manufactured to operate within the desired frequency range. Among the three antennas with stripline feed, only DETSA covers the whole 7250–7750 MHz range. However, the others can still be considered as operational for most of the satellites. When comparing the three antennas, DETSA has the widest bandwidth, lowest  $S_{11}$  value and smallest surface area. DETSA surface area is 27.5% less than the surface area of DLTSA. The designed DCTSA without the stripline feed can also be considered covering the whole 7250–7750 MHz range.

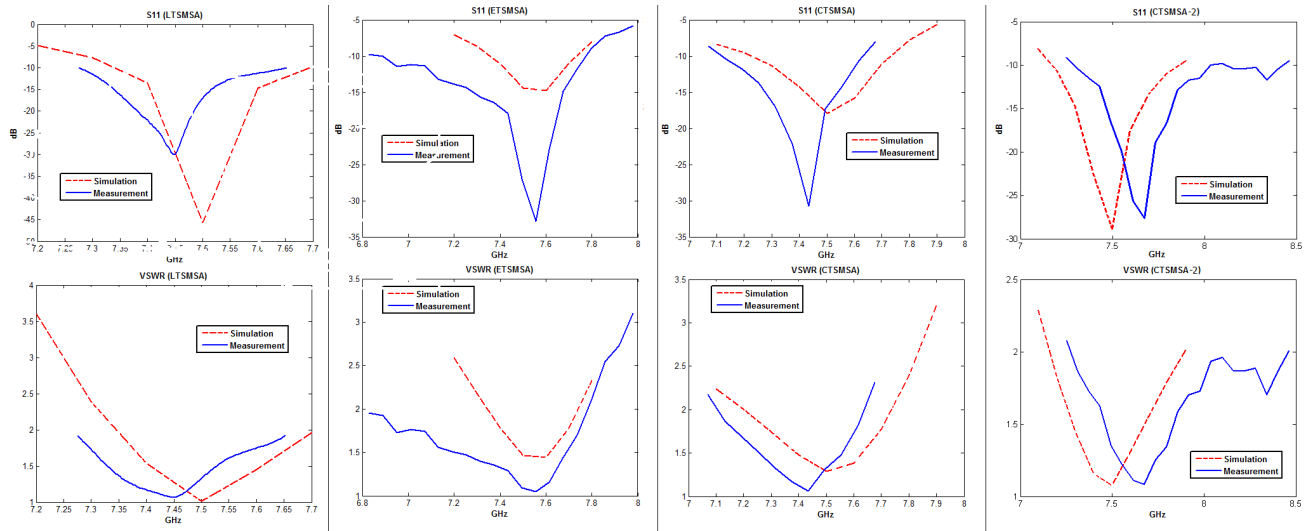


Figure 6. Simulated vs. measured  $S_{11}$  and VSWR values for TSAs.

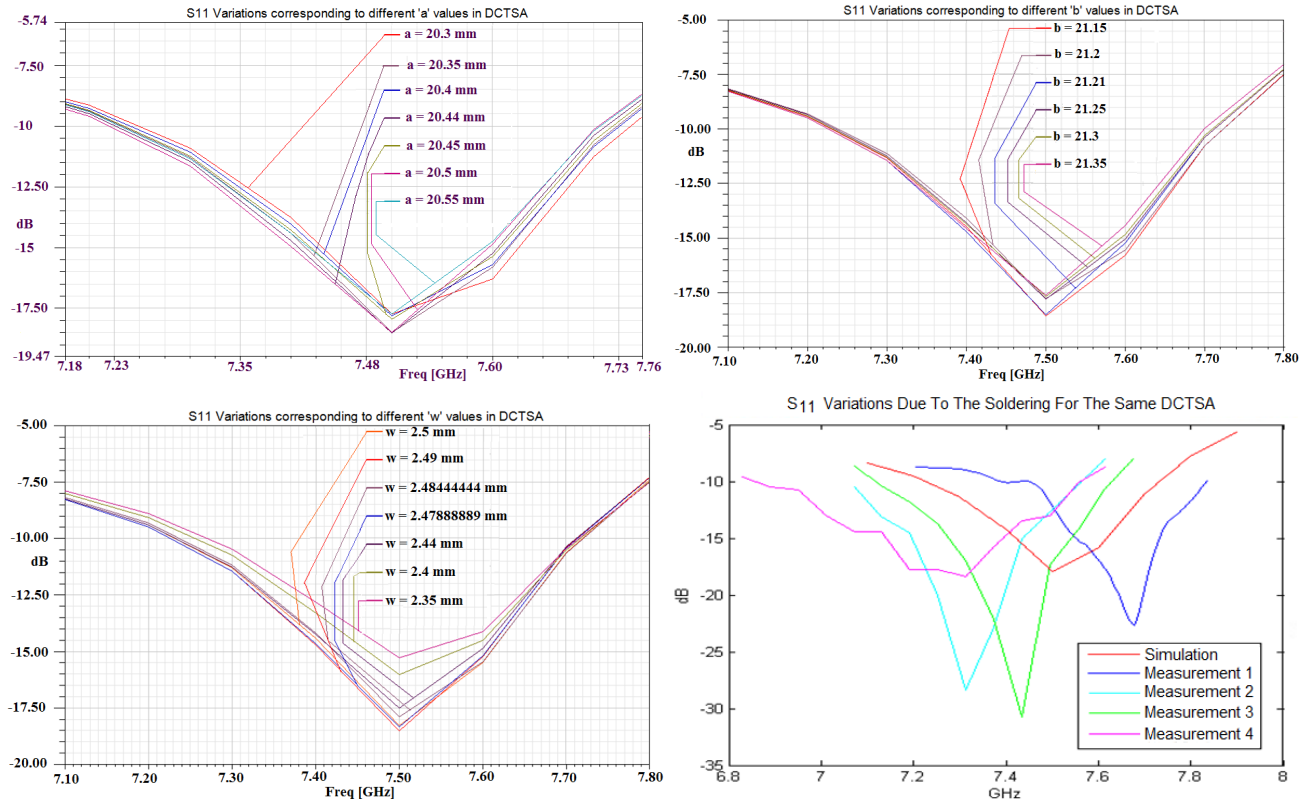


Figure 7.  $S_{11}$  simulation sensitivity to parameter deviations and variations due to DCTSA soldering.

Only  $S_{11}$  and VSWR values could be measured with the available equipment. It can be seen that there is similarity between the simulated and measured  $S_{11}$  values. All the measured center frequencies are inside 7250–7750 MHz range. But there exists some degree of relatively small deviation with respect to the expected 7500 MHz. During the simulations, it is observed that the small variations in antenna dimensions have a big impact on the antenna performance for all of the antennas. As seen in Figure 7,  $S_{11}$  variations, corresponding to 1/20 of mm changes in each parameter's value, can cause up to 3 dB difference. Therefore, manufacturing is done with CNC machines to obtain high precision. However, according to the measured  $S_{11}$  values, there are still some deviations in their center frequencies, with respect to 7500 MHz. The main reason for this phenomenon is believed to be the soldering process. For instance, four copies of the same DCTSA are manufactured, soldered, and  $S_{11}$  values are measured. It is surprising to see that even though the antennas have exactly the same dimensions, four different center frequencies are obtained, as shown in Figure 7. This kind of variations due to the manufacturing deviations makes it hard to conclude that the other design criteria are met without measuring with additional equipment. Nevertheless, the measured  $S_{11}$  values can be considered as promising, so it is still believed that the manufactured antennas are good candidates to be used as receiver antennas, which are capable of operating in X-Band Satellite Communications

## 5. CONCLUSION

Tapered slot antennas capable of operating in X-Band SATCOM range are presented in this paper. The antennas are defined in three parameters ( $a$ ,  $b$  and  $w$ ), and the optimum values for each parameter are calculated using GA tool in HFSS. The simulated antennas are then fabricated.  $S_{11}$  and VSWR measurement results show agreement with simulations.

Also, the newly introduced semi-annular stubs on both sides of the SMA connector are shown to be effective. In classical approach, TSAs are fed from one of their sides, parallel to their surfaces. This study uses a new feeding mechanism, which is perpendicular to the surfaces. By this approach, the manufactured antennas can be placed conformal to the surfaces of platforms, on which aerodynamic considerations are more important. Since the manufactured antennas are considerably smaller, lighter and much cheaper than conventional SATCOM receiver antennas, they can be used in UAVs or other airborne and space platforms. Since the required fabrication labor is minimal, and the required parts are fewer, greater reliability can be achieved.

Another achievement in this study is the newly introduced circularly tapering profile. In literature, there have been researches on linearly and exponentially tapering profiles. This study is the first instance of circularly tapering, which is shown to be promising for future works. Even though the radiation patterns are obtained by simulation, the evolved single-element DCTSA2 has an elevation coverage at least  $160^\circ$  (from  $10^\circ$  to  $170^\circ$ ) along with approximately  $90^\circ$  azimuth coverage (from  $-45^\circ$  to  $45^\circ$ ). The ranges are calculated according to the gain values greater than or equal to  $-5$  dBi, similar to that in the researches [13, 14]. With this high maximal elevation result, as the elevation angle relative to the ground changes, reliable performance and longer communication duration between satellite and ground terminals are achieved.

Additionally, by dual tapering profiles, the currents are confined to the tapering regions, which are narrow conductors. As a result, unwanted currents on other regions of the antennas are omitted.

A future research will be designing and optimizing a compact TSA with minimal surface. Although for DLTSAs it is not possible to be without the stripline feed, removing the 16 mm stripline feed insertion for DETSA, just as DCTSA, may further reduce the antenna dimensions. Another improvement will be increasing the beamwidth to obtain larger satellite coverage.

This work is on X-Band Satellite Communications; however, this approach can be extended to other research areas on mobile communications, as well. The same approach can be applied to design TSAs that are capable of operating in other frequency bands, such as complimentary portion of 5G, in which ample spectrum is available above 6 GHz.

## REFERENCES

1. Lewis, L. R., M. Fasset, and J. Hunt, "A broadband stripline array," *IEEE AP-S*, Vol. 12, 335–337, 1974.
2. Gibson, P. J., "The vivaldi aerial," *9th European Microwave Conference*, 101–105, Brighton, UK, IEEE, September 17–20, 1979.
3. Prasad, S. N. and S. Mahapatra, "A novel MIC slotline aerial," *9th European Microwave Conference*, 120–124, Brighton, UK, IEEE, September 17–20, 1979.
4. Gazit, E., "Improved design of a Vivaldi antenna," *IEE Proc.-H*, Vol. 135, 89–92, 1988.
5. Langley, J. D. S., P. S. Hall, and P. Newham, "Balanced antipodal vivaldi antenna for wide bandwidth phased arrays," *IEE Proceedings — Microwaves, Antennas and Propagation*, Vol. 143, 97–102, 1996.
6. Yngvesson, K. S., T. L. Korzeniowski, Y. S. Kim, E. L. Kollberg, and J. F. Johansson, "The tapered slot antenna — a new integrated element for millimeter-wave applications," *IEEE Transactions on Microwave Theory and Techniques*, Vol. 37, 365–374, 1989.
7. Fisher, J., "Design and performance analysis of a 1–40 GHz ultra-wideband antipodal vivaldi antenna," *German Radar Symposium GRS 2000*, Berlin, Germany, October 11–12, 2000.
8. Schiek, B. and J. Kohler, "An Improved microstrip-to-microslot transition," *IEEE Transactions on Microwave Theory and Techniques*, Vol. 24, 231–233, 1976.
9. Schuppert, B., "Microstrip/slotline transitions, modeling and experimental investigation," *IEEE Transactions on Microwave Theory and Techniques*, Vol. 36, 1272–1281, 1988.
10. Sloan, R., M. M. Zinieris, and L. E. Davis, "A broadband microstrip to slotline transition," *Microw. Opt. Techn. Let.*, Vol. 18, 339–342, 1998.
11. Erdoğan, Y., "Parametric study and design of vivaldi antennas and arrays," *MSc*, Middle East Technical University, Ankara, Turkey, 2009.
12. Jolani, F., G. Dadashzadeh, M. Naser-Moghadas, and A. Dadgarpour, "Design and optimization of compact balanced antipodal vivaldi antenna," *Progress In Electromagnetics Research*, Vol. 9, 183–192, 2009.
13. Lohn, J. D., G. S. Hornby, S. Gregory, A. Rodriguez-Arroyo, D. S. Linden, W. F. Kraus, and S. E. Seufert, "Evolutionary design of an X-band antenna for NASA's space technology 5 mission," *IEEE Antenna and Propagation Society International Symposium and USNC/URSI National Radio Science Meeting*, 2313–2316, Monterey, CA, USA, IEEE, June 20–25, 2004.
14. Hornby, G. S., A. Globus, D. S. Linden, and J. D. Lohn, "Automated antenna design with evolutionary algorithms," *American Institute of Aeronautics and Astronautics Space*, 19–21, 2006.
15. Lee, J. J. and S. Livingston, "Wide band bunny-ear radiating element," *Antennas and Propagation Society International Symposium*, Vol. 3, 1604–1607, Ann Arbor, Miami, USA, IEEE, June 28–July 02, 1993.
16. Weinschel, H. D., "Progress report on development of microstrip cylindrical arrays for sounding rockets," *Physics and Science Laboratory*, New Mexico State University, Las Cruces, 1973.
17. Sanford, G. G., "Conformal microstrip phased array for aircraft tests with ATS-6," *30th National Electronics Conference*, Vol. 9, 252–257, Chicago, Illinois, USA, October 16–18, 1974.
18. Simons, R. N., R. Q. Lee, and T. D. Perl, "Non-planar linearly tapered slot antenna with balanced microstrip feed," *Antennas and Propagation Society International Symposium*, Vol. 4, 2109–2112, Chicago, Illinois, USA, IEEE, June 18–25, 1992.
19. Lekshmi, B. S. K. and I. J. Raglend, "Parametric study of tapered slot antenna for wide band applications," *International Conference on Computation of Power, Energy, Information and Communication*, 71–77, Chennai, Tamil Nadu, India, IEEE, April 22–23, 2015.